Apoptosis (2019) 24:511–528
https://doi.org/10.1007/s10495-019-01535-x

BDNF-mediated mitophagy alleviates high-glucose-induced brain microvascular endothelial cell injury

Hong Jin[1] · Yi Zhu[1] · Yiping Li[1] · Xiuyu Ding[2] · Wenqi Ma[1] · Xiqiong Han[1] · Bilei Wang[1]

Published online: 15 March 2019

Abstract

Endothelial cell dysfunction and diabetic vascular complications are intrinsically linked. Although BDNF plays a protective role in cerebral microvascular complications caused by diabetes, the mechanisms of this activity are not fully clear. In this study, we investigated the role of BDNF in the hyperglycemic injury of BMECs and its associated intracellular signal transduction pathways. BMECs were treated with 33 mM glucose to imitate the endothelium under hyperglycemic conditions. The high-glucose treatment caused cell dysfunction, as evaluated by oxidative stress and cell apoptosis, which could be alleviated by BDNF. In addition, BDNF preserved mitochondrial function as assessed by mPTP opening, mitochondrial membrane potential, calcium content, and mitochondrial biogenesis markers. Western blot analysis of LC3-II, p62, and TOMM20 and the detection of mRFP-GFP-LC3 adenovirus for autophagy flux revealed that BDNF enhanced autophagy flux. Furthermore, BDNF activated mitophagy, which was confirmed by the observed colocalization of LC3-II with BNIP3 and from transmission electron microscopy observations. The HIF-1α/BNIP3 signaling pathway was associated with BDNF/TrkB-induced mitophagy. In addition, BDNF-induced mitophagy played a protective role against BMEC damage under hyperglycemia. Thus, the results of this study suggest that BDNF/TrkB/HIF-1α/BNIP3-mediated mitophagy protects BMECs from hyperglycemia.

Keywords BDNF · BMECs · Hyperglycemia · Mitochondrial function · Mitophagy

Abbreviations

BDNF	Brain-derived neurotrophic factor
BMECs	Brain microvascular endothelial cells
mPTP	Mitochondrial permeability transition pore
LC3-II	Microtubule-associated protein 1 light chain 3B
p62	SQSTM1
TOMM20	Translocase of outer mitochondrial membrane 20
HIF-1α	Hypoxia-inducible factor-1α
TrkB	Tropomyosin receptor or kinase B
BNIP3	BCL2/adenovirus E1B 19 kDa protein-interacting protein 3

Hong Jin and Yi Zhu have contributed equally to this study.

Electronic supplementary material The online version of this article (https://doi.org/10.1007/s10495-019-01535-x) contains supplementary material, which is available to authorized users.

✉ Hong Jin
220152975@seu.edu.cn

[1] Department of Cardiology, School of Medicine, Zhongda Hospital, Southeast University, Nanjing 210009, People's Republic of China

[2] Nanjing Ninghai Middle School, Nanjing 210009, People's Republic of China

Introduction

Diabetic cardiovascular complications are the leading cause of high morbidity and mortality in patients with diabetes [1]. Several studies have shown that diabetes can impair the function of small cerebral arteries and arterioles [2–4]. Brain microvascular endothelial injury is an important feature of cerebral vascular dysfunction [5, 6]. Hyperglycemia can enhance reactive oxygen species (ROS) generation, which subsequently causes the apoptosis of endothelial cells through the phosphatidylinositol-4,5-bisphosphate 3-kinase (PI3K)/protein kinase B (AKT)/nuclear factor kappa-light-chain-enhancer of activated B cells (NF-κB) signaling pathway [7]. Therefore, targeting excessive ROS generation is a key therapeutic approach for diabetic cerebral vascular complications. Furthermore, because damaged

mitochondria are the primary source of ROS formation [8–10], the focus of therapeutic approaches is to eliminate impaired mitochondria.

Mitochondria are double membrane-bound organelles that are essential for energy production and cellular homeostasis [11]. When cells undergo injury, the mitochondrial permeability transition pore (mPTP) opens, inducing calcium overload and membrane potential decline, which eventually causes decreased ATP production [12]. The elimination of damaged and unnecessary mitochondria is closely regulated by mitochondria-selective autophagy (mitophagy), which has a protective role in mitochondrial dysfunction and cell damage [13, 14].

Mature brain-derived neurotrophic factor (BDNF) together with its receptor tropomyosin receptor kinase B (TrkB) play vital roles in the central nervous system [15]. Recent studies have reported an association of BDNF with inflammatory conditions, such as coronary artery disease (CAD) and type 2 diabetes mellitus (T2DM) [16, 17]. We previously showed that decreased circulating BDNF levels are linked to endothelial dysfunction and that circulating BDNF levels have a cardiovascular prognostic value [18]. Wood, J. *et al*. suggested that BDNF can reduce body weight gain and partially alleviate metabolic abnormalities [19]. In the diabetic brain, a reduction in BDNF levels elevates the risk of brain microvascular endothelial cell (BMEC) injury for a variety of cerebrovascular diseases [20, 21]. Although these findings suggest an antidiabetic and anti-inflammatory role of BDNF, a comprehensive understanding of the relationship between the protective function of BDNF and endothelial cell injury under hyperglycemic conditions remains unclear.

Because damaged mitochondria-triggered ROS formation is tightly associated with endothelial cell dysfunction, in this study, we focused on BCL2/adenovirus E1B 19 kDa protein-interacting protein 3 (BNIP3)-mediated mitophagy, which is inhibited under high-glucose (HG) conditions [22]. BDNF/TrkB can induce vascular endothelial growth factor (VEGF) via hypoxia-inducible factor-1α (HIF-1α) in neuroblastoma cells [23]. In addition, BDNF/TrkB can protect retinoblastoma cells from apoptosis through HIF-1α activation [24]. Furthermore, the HIF-1α/BNIP3 signaling pathway has been reported to be important for hypoxia-induced autophagy and apoptosis [25–28]. Thus, we hypothesized that BDNF/TrkB/HIF-1α/BNIP3-mediated mitophagy could occur in the microcirculatory system of patients with diabetes, which could alleviate hyperglycemia-induced endothelium dysfunction.

In this study, we examined the ability of the BDNF/TrkB/HIF-1α/BNIP3 signal transduction pathway to regulate mitophagy in BMECs. We observed that BDNF alleviates the cell injury and mitochondrial dysfunction induced by HG treatment. BDNF activated autophagy flux and mitophagy, which involved the TrkB/HIF-1α/BNIP3 signaling pathway. Targeted decreases in BNIP3 expression weakened the ability of BDNF to protect BMECs from damage under hyperglycemia.

Materials and methods

Cell culture

Mouse BMECs (bEnd.3), which are somewhat similar to human BMECs [29], were obtained from Sciencell (Shanghai, China). Between passages 3 and 7, BMECs were cultured in Dulbecco's modified Eagle's medium (DMEM) containing a low concentration of glucose (5.5 mM) with 10% fetal bovine serum and antibiotics at 37 °C under an atmosphere with 5% CO_2.

Cell viability analysis

BMECs were seeded onto 96-well plates at a density of 5,000 cells/well for 24 h. The HG-induced damage model was established using a method described in previous studies [30]. To rule out effects caused by the high permeability of HG on cells, we used mannitol as a control. BMECs were cultured under normal-glucose (5.5 mM), hyperosmosis (5.5 mM glucose + 27.5 mM mannitol) or HG (33 mM) conditions for 12, 24, 48, and 72 h. After treatment, 10 μL of CCK-8 solution (Beyotime Biotechnology, Jiangsu, China) was added to each well, and the cells were incubated for 2 h at 37 °C. Subsequently, the absorbance of the samples was measured at a wavelength of 450 nm.

Detection of intracellular ROS

Intracellular ROS levels were measured using an oxidation-sensitive fluorescent probe, dihydroethidium (DHE) (Beyotime Biotechnology, Jiangsu, China). BMECs were washed twice with serum-free DMEM and then incubated in the dark with 10 μM DHE for an additional 30 min. Subsequently, the BMECs were rewashed twice, and DHE fluorescence was imaged using an FV10i confocal microscope (Olympus, Japan). At least 3–5 images per condition were analysed. The confocal images were quantified with Image J (Rawak Software, Inc., Germany).

Measurements of superoxide dismutase (SOD) activity, malondialdehyde (MDA) content, and nitric oxide (NO) content

BMECs were lysed with lysis buffer (Beyotime Biotechnology, Jiangsu, China) after which superoxide dismutase (SOD) activity and malondialdehyde (MDA) content were

measured according to the manufacturer's protocol (Beyotime Biotechnology, Jiangsu, China) and normalized to the total protein content with a bicinchoninic acid (BCA) protein assay kit (KeyGEN Biotechnology, Jiangsu, China). The nitric oxide (NO) content in the cell supernatants was detected using an NO assay kit according to the manufacturer's protocol (Beyotime Biotechnology, Jiangsu, China).

Annexin V-FITC/propidium iodide (PI) detection of apoptosis

The early apoptosis of BMECs was determined using an annexin V-FITC/propidium iodide (PI) apoptosis detection kit (Solarbio Biotechnology, Beijing, China) according to the manufacturer's instructions. Approximately 1×10^5 cells from each group were collected, washed twice with cold PBS, and then stained using annexin V-FITC/PI in dark. The number of necrotic (Q1), late apoptotic (Q2), early apoptotic (Q3), and living cells (Q4) were quantified using a flow cytometer (BD Biosciences, USA). The early apoptosis rate (%) was calculated as (the number of early apoptotic cells / the number of total cells) × 100%.

Mitochondrial isolation

Mitochondrial and cytosolic fractions were obtained using a mitochondrial isolation kit (Beyotime Biotechnology, Jiangsu, China). Mitochondrial fractions were separated according to the manufacturer's instructions. Briefly, after the BMECs were incubated in ice-cold mitochondrial lysis buffer for 15 min, the cell suspension was homogenized for 20 strokes. Next, the homogenate was centrifuged at 1000×*g* for 10 min at 4 °C to remove the nuclei and unbroken cells. The supernatant was then collected and centrifuged again at 11,000×*g* for 10 min at 4 °C to obtain the mitochondrial fraction. For western blotting, the mitochondrial fractions were stored in mitochondrial lysis buffer containing PMSF.

Mitochondrial function analysis

mPTP opening was measured using a mPTP colorimetric detection kit (Genmed Scientifics Inc., Shanghai, China). The relative fluorescence units of mitochondrial volume changes were recorded using a spectrophotometer (MULTISKAN GO, Thermo Fisher Scientific, USA).

The mitochondrial calcium content was detected using a mitochondrial calcium probe (Fluo-4 AM, Molecular Probes) (Beyotime Biotechnology, Jiangsu, China) and a confocal microscope (Olympus). At least 3–5 images per condition were analysed.

The mitochondrial membrane potential was evaluated via JC-1 staining (KeyGEN Biotechnology, Jiangsu, China) using a flow cytometer (BD Biosciences, USA). BMECs with healthy mitochondria were distributed in Q2, while BMECs with decreased mitochondrial membrane potential were distributed in Q3.

The ATP levels in BMECs were detected using an ATP assay kit (Beyotime Biotechnology, Jiangsu, China) according to the manufacturer's protocol, with luminescence measured using a microplate reader (Bio-Rad, Shanghai, China).

Measurement of mitochondrial DNA copy number

The mitochondrial DNA copy number was assessed by determining the amplicon ratio from PCR using specific primers against a gene encoded by mitochondrial DNA [NADH dehydrogenase subunit 2 (ND2)] and a gene encoded by nuclear DNA (β-actin). Total DNA was isolated from the cells, and the quantification of mitochondrial and genomic genes was performed by qRT-PCR. The forward and reverse primers are listed in Table 1. Fifteen nanograms of cDNA and the primer sets (200 nM each) were used for each reaction. Relative ND2 and β-actin values within each sample were used to obtain a ratio.

Transfection and transduction

To silence HIF-1α and BNIP3, small interfering RNAs (siRNAs) were designed (Shanghai Genechem Co. Ltd.). The siRNAs were transfected into cells using Lipofectamine 2000 (Invitrogen Life Science, Grand Island, NY) according to the manufacturer's protocol, and the silencing efficiency was examined by western blotting.

To assess autophagy flux, BMECs were transduced with mRFP-GFP-LC3 double-labeled adenovirus (Shanghai Hanbio Biotechnology Co. Ltd.) for 6 h, after which the medium was replaced with fresh low-glucose complete medium. At 48 h after transfection, the cells were cultured with or without BDNF under normal-glucose or HG conditions for 24 h, and autophagosomes (yellow) and autolysosomes (red) were subsequently detected using a confocal microscope (Olympus, Japan). At least 5–7 images per condition were analysed.

Table 1 Primer sequences for the mitochondrial DNA copy number analysis

Genes	Primer sequences
ND2	Forward, 5′-CACAGAAGCTGCCATCAAGTA-3′
	Reverse, 5′- CCGGAGAGTATATTGTTGAAGAG-3′
β-actin	Forward, 5′-CCATGTTCCAAAACCATTCC-3′
	Reverse, 5′-GGGCAACCTTCCCAATAAAT-3′

Quantitative reverse transcriptase-polymerase chain reaction (qRT-PCR)

Total RNA was isolated from cells according to the manufacturer's instructions. RNA purity was evaluated based on the A260/A280 ratio, which was determined using a Merinton SMA4000 system. Reverse transcription (RT) was performed with Prime Script TM Master Mix (Takara). qRT-PCR was performed with a StepOnePlus instrument (ABI) using SYBR Green Mix and the PCR primers listed in Table 2. The results were normalized to the expression levels of β-actin.

ELISA

ELISA (Promega, USA) with a sensitivity of < 80 pg/ml was performed to measure the BDNF levels in cell supernatants and lysates according to the manufacturer's protocols. The standards or samples were added to each well, and after incubating for 1 h at 37 °C, each well was washed and incubated for another 30 min at 37 °C with the indicated antibodies. The absorbance at 450 nm was measured with a microplate reader (Bio-Rad). The results were standardized to the cell number in each well.

Western blotting

BMECs were lysed using a nuclear and cytoplasmic protein extraction kit purchased from Beyotime Biotechnology according to the manufacturer's instructions, and the protein concentration in the lysates was measured using a BCA protein assay kit. To assess the purity of the cell fractions, we measured the levels of β-actin and Lamin B1 protein in the nuclear and cytoplasmic fractions, respectively (Supplementary Fig. 1), the results of which demonstrated that the cell fractions exhibited good purity. Antibodies against HIF-1α (CST36169) (1:1000), microtubule-associated protein 1 light chain 3 (LC3) (CST4108) (1:1000), SQSTM1 (p62) (CST23214) (1:500), cleaved caspase-3 (CST9661) (1:1000), cleaved caspase-9 (CST9509) (1:1000), Bcl-2 (CST3498) (1:1000), and Bax (CST14796) (1:1000) were obtained from Cell Signaling Technology (Danvers, MA, USA). Anti-BDNF (ab108319) (1:2000), anti-BNIP3 (ab109362) (1:1000), anti-translocase of outer mitochondrial membrane 20 (TOMM20) (ab186734) (1:500), anti-peroxisome proliferator-activated receptor gamma coactivator 1-alpha (PGC-1α) (ab54481) (1:1000), anti-nuclear respiratory factor 1 (NRF-1) (ab175932) (1:1000), anti-nuclear factor (erythroid-derived 2)-like 2 (NRF-2) (ab137550) (1:500), anti-mitochondrial transcription factor A (TFAM) (ab131607) (1:2000), anti-Lamin B1 (ab16048) (1:1000), anti-dynamin-related protein 1 (Drp1) (ab184247) (1:1000), and anti-voltage-dependent anion channel 1 (VDAC1) (ab154856) (1:2000) antibodies were purchased from Abcam (Cambridge, MA, USA). Anti-β-actin (1:3000) and all secondary antibodies (1:5000) were provided by Biosharp (Anhui, China). In our study, internal reference proteins and targeted proteins were measured in sister membranes. For molecules above 70 kDa, we used 8% of SDS gels for electrophoresis, and for molecules below 70 kDa, we used 12% of SDS gels for electrophoresis. Subsequently, 40–60 μg of protein was loaded onto an SDS-PAGE gel and then transferred onto nitrocellulose membranes. The membranes were blocked with 5% nonfat milk for 1.5 h. The membranes were incubated with different primary antibodies overnight at 4 °C and then visualized using anti-rabbit or anti-mouse IgG conjugated with horseradish peroxidase for 1 h at room temperature. The blots were detected using electrochemiluminescence (ECL), and the results were quantified using Image-Pro Plus 6.0 (Media Cybernetics, Rockville, MD).

Table 2 Primer sequences for the qRT-PCR analysis

Genes	Primer sequences
BDNF	Forward, 5′-GCCCAACGAAGAAAACCATAAG-3′
	Reverse, 5′-GTTTGCGGCATCCAGGTAATT-3′
NRF-1	Forward, 5′-CTGATGGCACTGTCTCACTTATCC-3′
	Reverse, 5′-CCACGGCAGAATAATTCACTTG-3′
NRF-2	Forward, 5′-GCAGGCCAAGATGACGAAGT-3′
	Reverse, 5′-ACTTACACCGGCTCGGAGAA-3′
PGC-1α	Forward, 5′-CACACACAGTCGCAGTCACAAC-3′
	Reverse, 5′-CACACTTAAGGTGCGTTCAATAGTC-3′
TFAM	Forward, 5′-GGTCTGGAGCAGAGCTGTGC-3′
	Reverse, 5′-TGGACAACTTGCCAAGACAGAT-3′
β-actin	Forward, 5′-GGCTGTATTCCCCTCCATCG-3′
	Reverse, 5′-CCAGTTGGTAACAATGCCATGT-3′

Immunofluorescence staining

BMECs were fixed with 4% paraformaldehyde, permeabilized with 0.1% Triton X-100 for 20 min, and then blocked with 5% bovine serum albumin (BSA) for 0.5 h at room temperature. Anti-LC3 (1:500), anti-lysosomal-associated membrane protein 1 (LAMP1) (1:500) (Abcam, Cambridge, MA, USA), anti-BNIP3 (1:500), and anti-BDNF (1:500) antibodies were incubated with the cells at 4 °C overnight, after which the cells were incubated with the appropriate secondary antibodies for 0.5 h in the dark. Subsequently, the nuclei were stained with DAPI for 15 min, and images were obtained using a confocal microscope (Olympus, Japan). At least 3–5 images per condition were analysed.

Transmission electron microscopy (TEM)

Cells were fixed in 2.5% glutaraldehyde (electron microscopy grade) at 4 °C for 2 h, dehydrated in an ethanol series and embedded in Epon resin. Representative areas were chosen to generate ultrathin sections, which were viewed using a Hitachi transmission electron microscopy (TEM) system at an accelerating voltage of 80 kV. Digital images were obtained using an AMT imaging system (Advanced Microscopy Techniques Co., Danvers, MA, USA).

Statistical analysis

All of the experiments were independently repeated at least three times. All data are presented as the mean ± standard deviation (SD). Statistical analyses were performed using Statistical Package for Social Science (SPSS) 22.0 (SPSS, Chicago, IL, USA). Two-tailed Student's *t*-tests and one- or two-way ANOVA with post hoc comparisons by Tukey's multiple comparisons test were used to compare the results. Values of $P < 0.05$ were considered significant.

Results

HG induces BMEC injury

BMECs were cultured under normal-glucose (con) (5.5 mM), hyperosmosis (5.5 mM glucose + 27.5 mM mannitol), or HG (33 mM) conditions. The CCK-8 assay results showed that compared with the control groups, HG inhibited cell viability after 24, 48, and 72 h of treatment, and there was statistically significant time-dependence between the cell viability (Fig. 1a). Thus, the 24-h treatment was used for subsequent studies of HG-induced BMEC injury. High oxidative stress refers to elevated intracellular levels of ROS, and HG has been shown to increase intracellular ROS production [7, 31]. Our results showed that intracellular ROS formation and the MDA content were markedly elevated after HG treatment compared with those of the control groups, whereas the opposite trend was observed for SOD activity and NO content (Fig. 1b–e), suggesting the presence of high oxidative stress. Because excessive ROS generation contributes to cell apoptosis, we next performed annexin V-FITC/PI double staining and evaluated the levels of apoptosis pathway-related markers to assess apoptosis in BMECs after HG treatment. Caspases play a central role in the regulation and execution of apoptosis, where caspase-3 stimulates the final step in apoptosis, while Bcl-2 and Bax are key regulators of apoptosis [32]. As shown in Fig. 1f, the incubation of BMECs with HG led to enhanced early cell apoptosis and decreased healthy cell populations. The results shown in Fig. 1g also demonstrated that the HG treatment elevated proapoptosis protein levels (cleaved caspase-3, cleaved caspase-9, and Bax), whereas it diminished antiapoptosis protein expression (Bcl-2). In addition, the Bcl-2/Bax ratio was significantly decreased in the HG group. Taken together, these results demonstrated that HG causes excessive intracellular ROS generation and BMEC apoptosis, whereas the hypertonic treatment did not cause significant cell damage.

HG suppresses BDNF expression

To investigate the changes in BDNF expression under hyperglycemia, BMECs were treated with HG for 0, 6, 12, 24, and 48 h. The results showed that the levels of BDNF monomers and dimers, as assessed by western blotting, and total BDNF levels in BMEC lysates and supernatants, as assessed by ELISA, were decreased in the HG-treated groups compared with the control groups, and the maximum decrease was observed after 24 h of stimulation (Fig. 2a, b). These results were also confirmed by qRT-PCR (Fig. 2c). These results, together with the cell viability results described above, prompted us to use the 24-h treatment for all subsequent studies.

To further elucidate the association between decreased BDNF expression and the HG treatment, BMECs were incubated under normal-glucose or HG conditions for 24 h, after which the distribution of BDNF in cells was visualized by immunofluorescence staining. The results indicated that HG significantly inhibits BDNF translocation into the nucleus when compared with the control cells (Fig. 2d). Measuring the nuclear/cytoplasmic molecular ratio is also useful in assessing molecular nuclear translocation [33], and the western blot results showed that the HG treatment decreased the nuclear/cytoplasmic BDNF (dimer) ratio (Fig. 2e), further supporting the presence of a nuclear translocation block. Taken together, these results indicate that BDNF expression was decreased both transcriptionally and translationally during hyperglycemia-induced BMEC damage.

BDNF plays a protective role in HG-induced BMEC dysfunction

BDNF has been reported to have anti-inflammatory and antidiabetes roles. To demonstrate that BMECs cultured under HG conditions are protected by BDNF, we treated cells with recombinant human BDNF protein (100 ng/ml) (Abcam, Cambridge, MA, USA), which has been shown to be stable during cell culture [34, 35]. The CCK-8 assay results indicated that BDNF significantly alleviated the HG-induced decrease in cell viability compared with that observed in the untreated HG group (Fig. 3a). In addition, BDNF exhibited antioxidative stress effects, as evaluated by intracellular ROS formation, SOD activity,

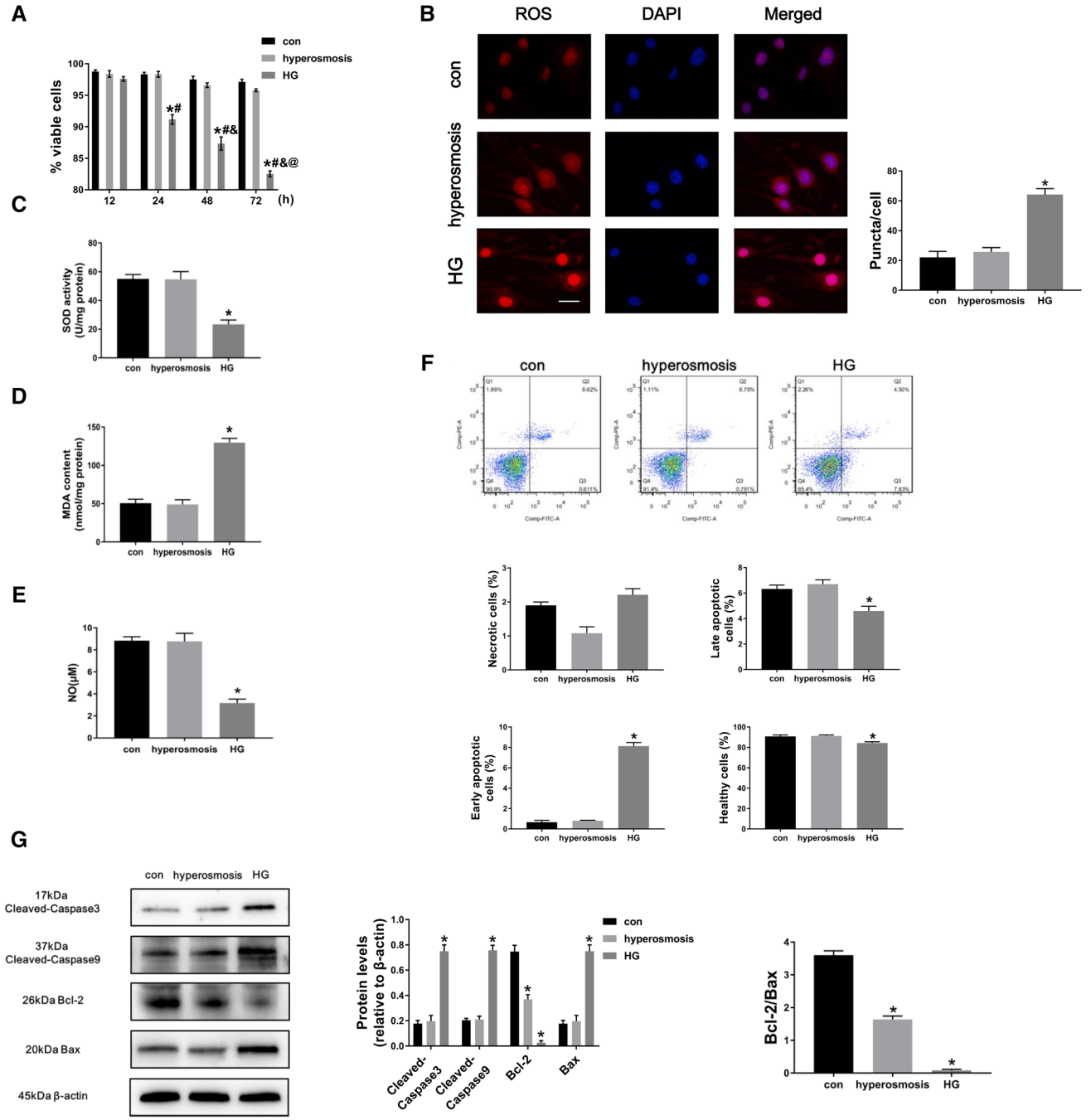

Fig. 1 HG induces BMEC dysfunction. BMECs were cultured under normal glucose (con) (5.5 mM), hyperosmosis (5.5 mM glucose + 27.5 mM mannitol), or high-glucose (HG) (33 mM) conditions. **a** After 0, 12, 24, 48, and 72 h of treatment, cell viability was assessed through a CCK-8 assay. **b** ROS production was measured by immunofluorescence with confocal microscopy after 24 h. Scale bar, 10 μm. $*P<0.05$ compared with the control group at each time point. $\#P<0.05$ compared with the HG group at 12 h. $\&P<0.05$ compared with the HG group at 24 h. $@P<0.05$ compared with the HG group at 48 h. **c–e** SOD activity, MDA content, and NO content were determined after 24 h of treatment. $*P<0.05$ compared with the control group. **f** After 24 h of incubation, healthy, early apoptotic, late apoptotic, and necrotic cell populations were evaluated by annexin V-FITC/PI double staining. $*P<0.05$ compared with the control group. **g** Protein levels of apoptosis pathway-related proteins. $*P<0.05$ compared with the control group. For **a**, two-way ANOVA with post hoc comparisons by Tukey's multiple comparisons test was used. For **b–g**, one-way ANOVA with post hoc comparisons by Tukey's multiple comparisons test was used

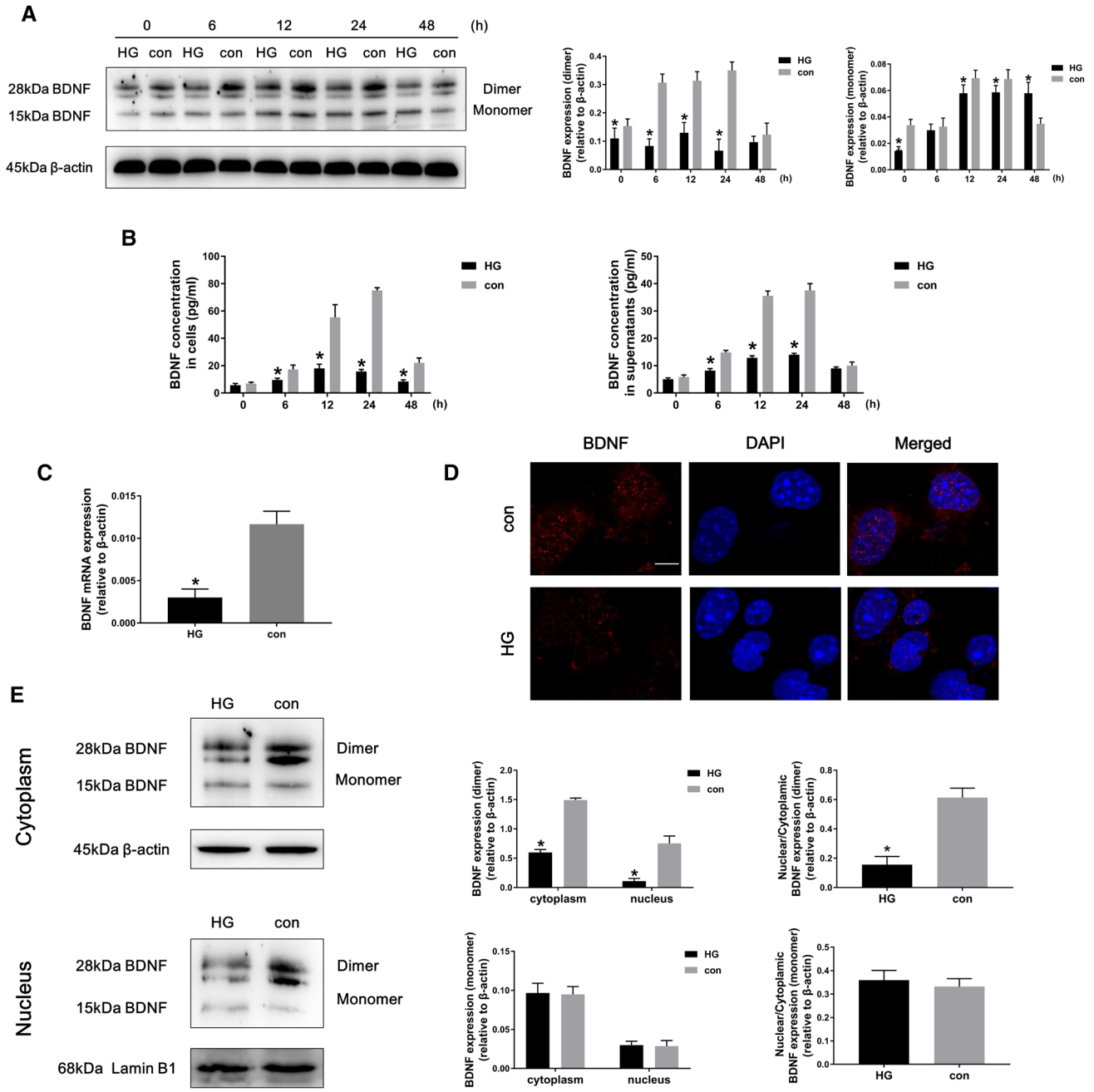

Fig. 2 HG inhibits BDNF transcriptional and translational expression. **a, b** BMECs were cultured under normal glucose or HG conditions, and monomeric and dimeric BDNF protein levels in BMECs were assessed by western blotting. BDNF in cell lysates and supernatants was detected by ELISA. **c** After cells were cultured for 24 h under normal glucose or HG conditions, BDNF mRNA levels were determined by qRT-PCR. **d, e** BDNF nuclear translocation in cells cultured under normal glucose or HG conditions for 24 h was evaluated by immunofluorescence with confocal microscopy and western blotting to assess nuclear/cytoplasmic BDNF (dimer and monomer) protein levels. Scale bar, 5 μm. For **a, b**, two-way ANOVA with post hoc comparisons by Tukey's multiple comparisons test was used. For **c, e**, two-tailed Student's *t*-test was used. $*P < 0.05$ compared with the control group

MDA content, and NO content (Fig. 3b–e). As expected, the results of the annexin V-FITC/PI double staining assay (Fig. 3f) and measurements of apoptosis pathway-related protein levels (Fig. 3g) showed that BDNF suppressed BMEC early apoptosis after HG exposure. In the HG + BDNF group, late cell apoptosis increased significantly, but the total number of healthy cells increased slightly. Although the increase was not statistically significant compared with the HG group, the decrease in early apoptosis combined with the changes in apoptosis

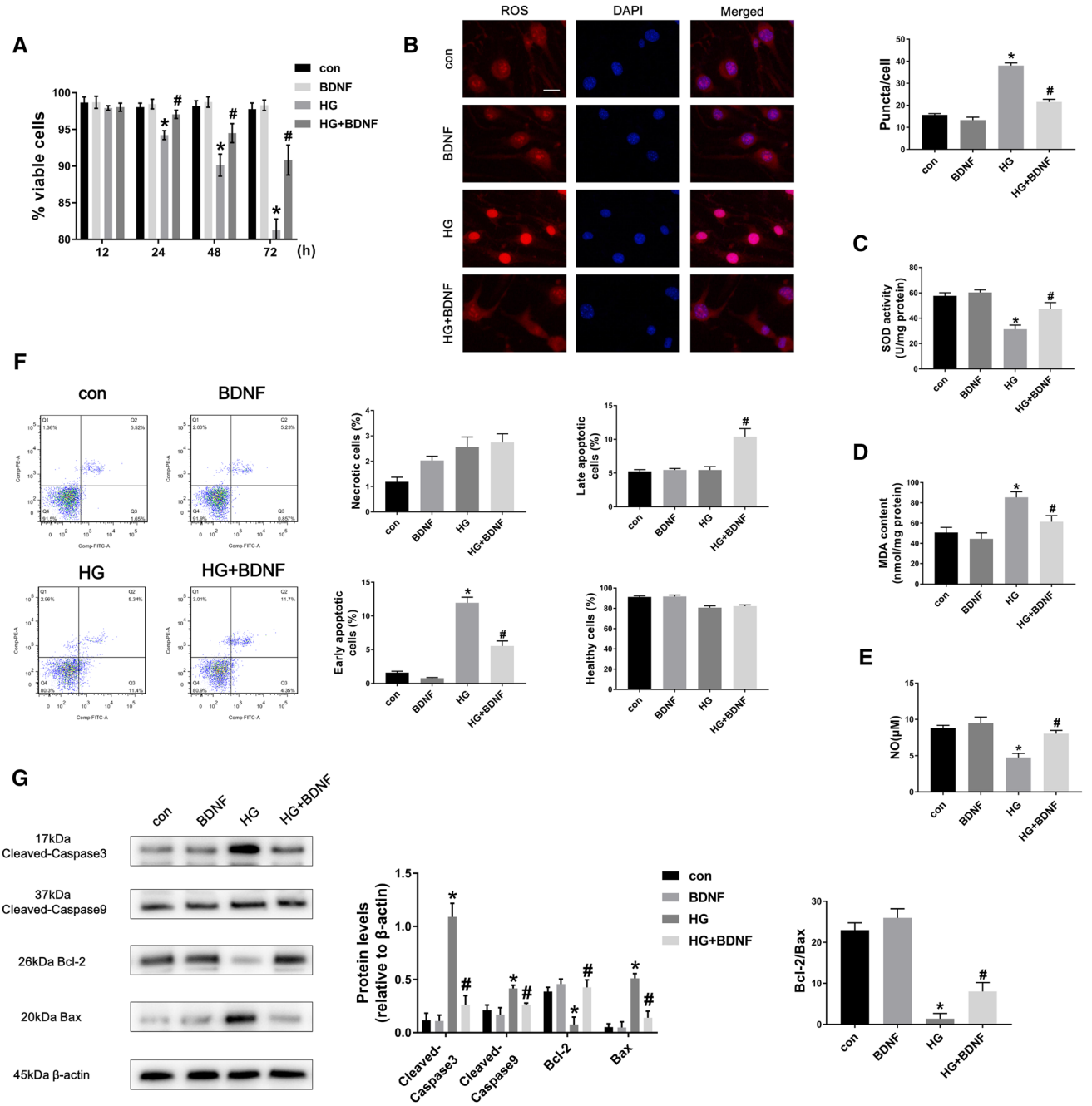

Fig. 3 BDNF alleviates BMEC damage under hyperglycemia. **a** BMECs were cultured under normal glucose or HG conditions in the presence or absence of BDNF (100 ng/ml), and cell viability was assessed through a CCK-8 assay at different time points. **b–e** After 24 h of treatment, ROS production, SOD activity, MDA content, and NO content were determined. Scale bar, 10 μm. **f** Healthy, early apoptotic, late apoptotic, and necrotic cell populations were evaluated by annexin V-FITC/PI double staining. **g** Protein levels of apoptosis pathway-related proteins. For **a**, two-way ANOVA with post hoc comparisons by Tukey's multiple comparisons test was used. For **b–g**, one-way ANOVA with post hoc comparisons by Tukey's multiple comparisons test was used. $*P < 0.05$ compared with the control group. $\#P < 0.05$ compared with the HG group

pathway-related protein levels also indicates the anti-apoptotic role of BDNF in the HG environment. All these results strongly suggest that BDNF can protect BMECs from HG damage.

BDNF preserves mitochondrial function

Since we showed that HG conditions can cause excessive cellular oxidative stress and apoptosis and since these

processes originate in the mitochondria [36], we explored the effects of BDNF treatment on mitochondrial function. The HG treatment resulted in an increased rate of mPTP opening, leading to decreased mitochondrial membrane potential and overloaded mitochondrial calcium levels compared with the control group. In contrast, the BDNF treatment suppressed mitochondrial swelling, thereby maintaining mitochondrial membrane potential and decreasing the mitochondrial calcium content (Fig. 4a–c). The primary role of mitochondria in cells is the production of energy. Our results revealed that

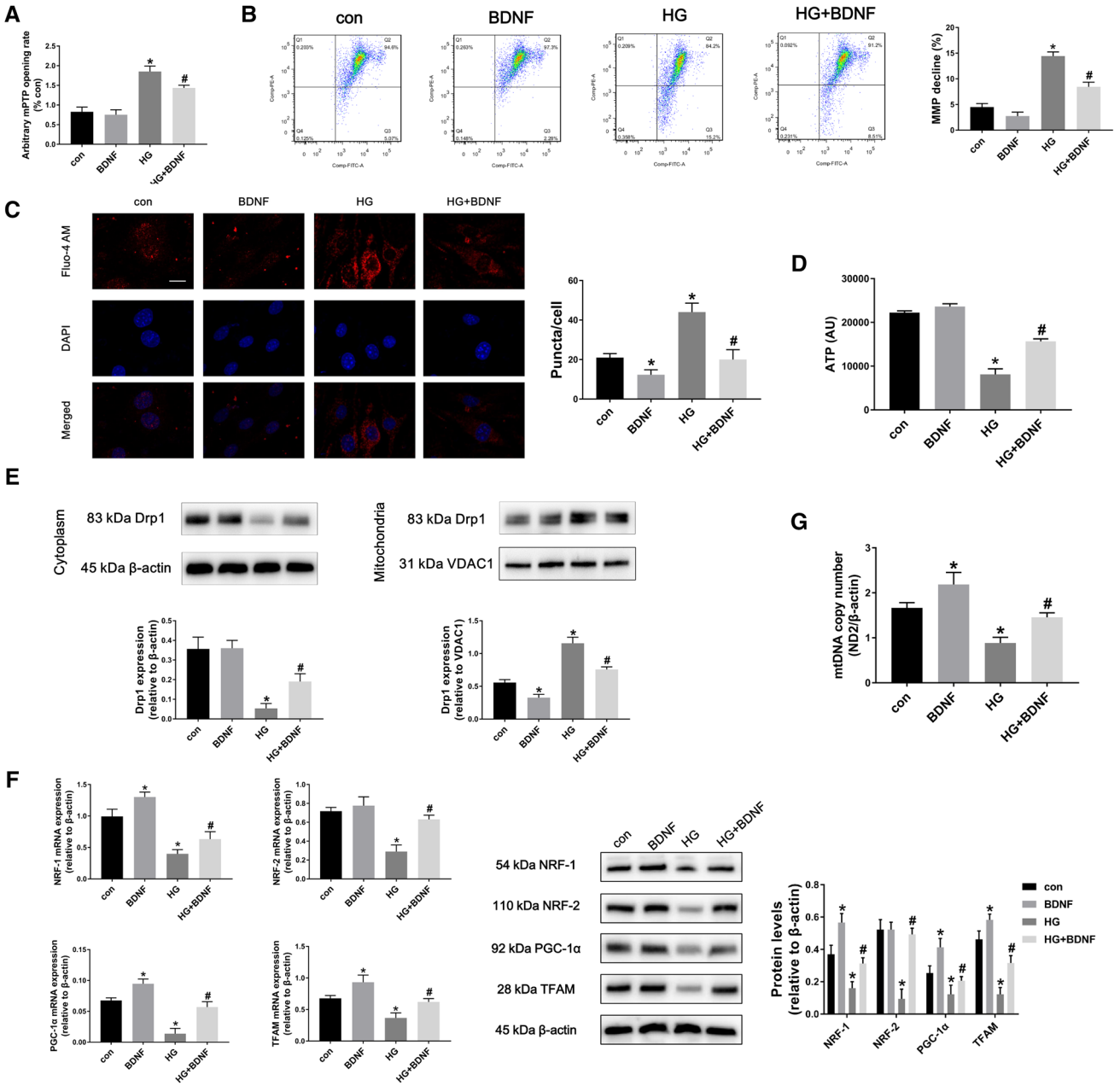

Fig. 4 BDNF preserves mitochondrial function. BMECs were cultured under normal glucose or HG conditions for 24 h in the presence or absence of BDNF (100 ng/ml). **a** The arbitrary rate of mPTP opening was evaluated by measuring the absorbance of samples at 505 nm. **b** The mitochondrial membrane potential was measured via JC-1 staining with flow cytometry. **c** The mitochondrial calcium levels were determined using the probe Fluo-4 AM with immunofluorescence detection. Scale bar, 10 μm. **d** Intracellular ATP levels were detected. **e** Cytoplasmic and mitochondrial Drp1protein levels were detected by western blotting. **f** The mRNA and protein levels of mitochondrial biogenesis markers. **g** The mitochondrial mass, as evaluated by determining the mitochondrial DNA copy number, was determined by qRT-PCR. This figure, one-way ANOVA with post hoc comparisons by Tukey's multiple comparisons test was used. $^{*}P < 0.05$ compared with the control group. $\#P < 0.05$ compared with the HG group

BDNF could alleviate the hyperglycemia-decreased intracellular production of ATP (Fig. 4d), suggesting a protective role of BDNF in HG-induced mitochondrial dysfunction. Because the integrity of the mitochondrial structure is crucial for the stabilization of mitochondrial function [37], we assessed the modification of the mitochondrial fission marker Drp1 through western blotting. The results showed that the HG treatment promoted Drp1 translocation to the surface of mitochondria for mitochondrial fission, whereas BDNF alleviated this tendency (Fig. 4e).

Because excessive mitophagy in the absence of mitochondrial biogenesis can damage mitochondrial function [38], we examined the mRNA and protein levels of mitochondrial biogenesis markers, including PGC-1α, NRF-1, NRF-2, and TFAM. All of these markers, which are important for the replication of mitochondrial DNA and the transcription of nuclear-encoded genes [39], were observed to be significantly upregulated in response to the BDNF treatment through qRT-PCR and western blot analysis of the whole cell lysates (Fig. 4f). To further confirm the effects of BDNF on mitochondrial biogenesis, we examined the mitochondrial mass in cells, which was also increased after the BDNF treatment (Fig. 4g). Taken together, these results suggest that BDNF contributes to mitochondrial biogenesis.

BDNF activates autophagy flux and mitophagy in BMECs

Mitophagy is a specific type of autophagy considered to be a repair mechanism for damaged mitochondria. Thus, we next assessed the effects of BDNF on autophagy flux. Compared with the untreated group, the BDNF treatment group exhibited increased LC3-II protein levels and decreased p62 levels, indicating that BDNF alleviated autophagy flux inhibition. Unexpectedly, the HG group did not exhibit significantly inhibited autophagy flux (Fig. 5a). To further evaluate the alterations in autophagy flux caused by BDNF, BMECs were transduced with mRFP-GFP-LC3 adenovirus and then treated with or without BDNF after culturing under normal-glucose or HG conditions for 24 h. We observed that the numbers of GFP (green) and mRFP (red) puncta were significantly increased after BDNF treatment and that greater numbers of yellow and red puncta were observed in cells treated with BDNF compared to the untreated cells, indicating an increase in the formation of both autophagosomes and autolysosomes. However, in the HG treatment group, only yellow puncta were observed, suggesting that autophagosomes were not degraded by lysosomes (Fig. 5b). To assess whether BDNF could alleviate the block in autophagosome and lysosome fusion, LC3-II and LAMP1 were double stained. After BDNF treatment, the LC3-II- and LAMP1-stained puncta exhibited an uneven distribution throughout the cells, and the extent of their colocalization was higher in the BDNF-treated group than in the untreated group (Fig. 5c). Thus, these results suggest that BDNF can enhance autophagy flux under normal-glucose and HG conditions.

We next investigated the changes in mitophagy mediated by BDNF. The levels of TOMM20 protein (a translocase of outer mitochondrial membrane) were observed to decrease after cells were incubated with BDNF for 24 h compared with those observed in the non-BDNF group, indicating the occurrence of enhanced mitochondrial clearance (Fig. 5a). In addition, the fusion of LC3-II and BNIP3 was enhanced by the BDNF treatment compared with the HG treatment (Fig. 6a), suggesting the formation of mitophagosomes. TEM was performed to obtain direct evidence of mitophagy, and as shown in Fig. 6b, at high magnification, the presence of increased numbers of autophagosomes with double-membrane structures containing swelled and dilated mitochondria (white arrows) was observed in the BDNF-treated group compared to the untreated group.

BDNF/TrkB induces mitophagy through the HIF-1α/BNIP3 signaling pathway

BDNF has a high affinity to the TrkB receptor [40], and BNIP3 acts as a receptor for targeting autophagosomes to mitochondria [41]. To investigate whether HIF-1α/BNIP3 signaling occurs during BDNF/TrkB-activated mitophagy, cells were treated with K-252a (Sigma-Aldrich, Saint Louis, USA), a potent TrkB inhibitor, and siRNAs against HIF-1α and BNIP3. BMECs were treated with or without BDNF under normal-glucose or HG conditions for 24 h, and the results showed that HIF-1α and BNIP3 protein levels were increased in the BDNF treatment group compared with those observed in the untreated group (Fig. 7a). The reason why HIF-1α was not significantly different between the BDNF group and the HG + BDNF group may be due to the amount of BDNF added. The concentration we used was 100 ng/ml according to the literature [42, 43] and the CCK-8 results (not included in the article); this concentration may cover the effect of the HG intervention. Next, we incubated BMECs with K-252a in the presence of BDNF, the results of which showed that K-252a treatment can inhibit HIF-1α expression in BMECs (Fig. 7b), suggesting a connection between TrkB and HIF-1α. For the HIF-1α knockdown assays, BMECs were transfected with siRNA against HIF-1α for 48 h, and the silencing efficiency examined by western blotting showed an approximately 70% decrease in HIF-1α protein levels compared with that observed in the scrambled siRNA groups (Supplementary Fig. 2a). Western blotting showed that silencing HIF-1α markedly downregulated BNIP3 protein levels under HG + BDNF conditions (Fig. 7c), however, there is no significant effect in normal state and HG state (data not shown). For BDNF to protect BMECs against HG-induced

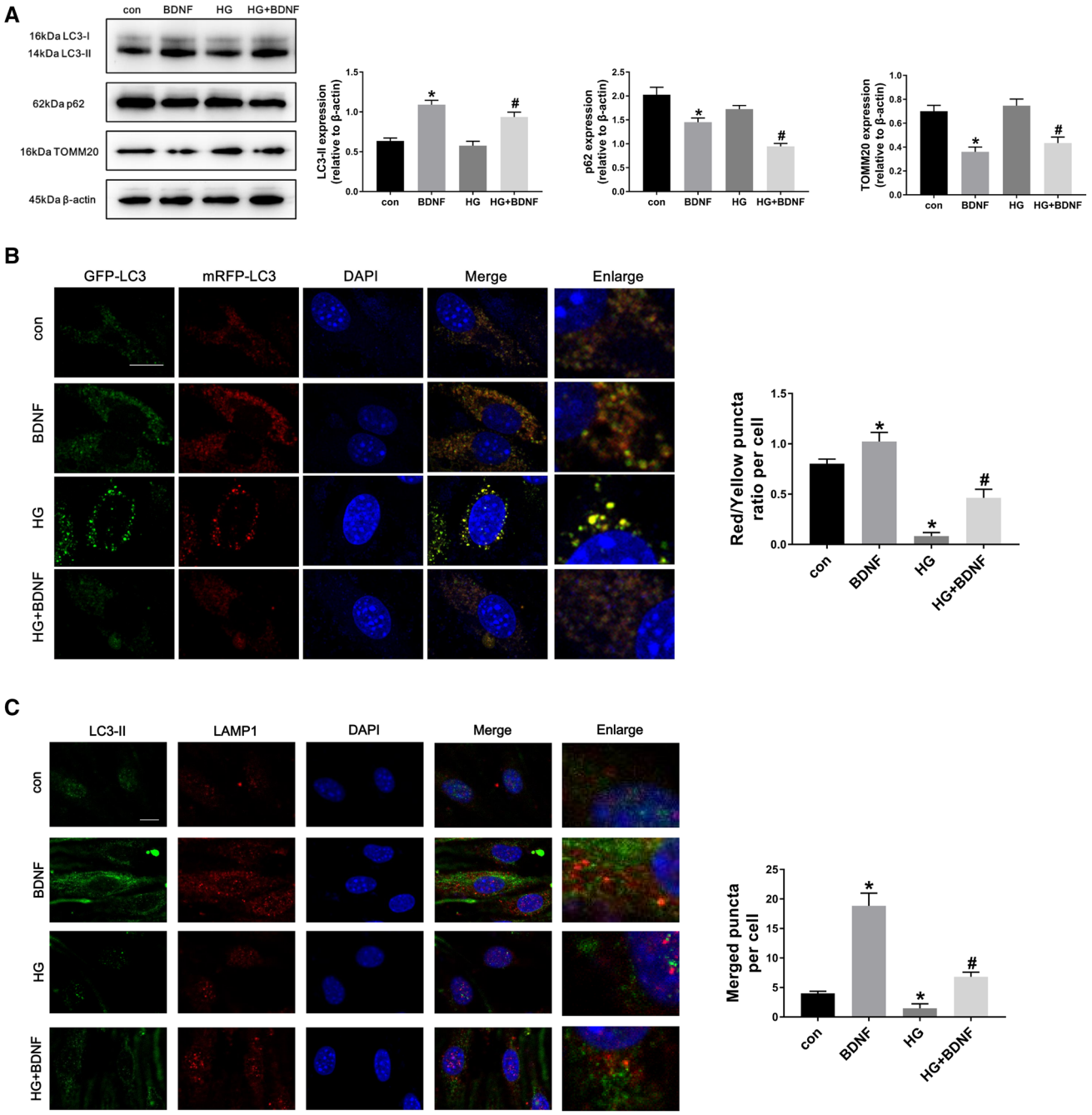

Fig. 5 BDNF enhances autophagy flux in BMECs. **a** Western blot analysis of LC3, p62, and TOMM20 protein levels with or without BDNF treatment (100 ng/ml) in cells cultured under normal glucose or HG conditions. **b** Fluorescence analysis of BMECs transfected with mRFP-GFP-LC3 adenovirus and then treated with or without BDNF (100 ng/ml) after normal glucose or HG exposure. The yellow puncta indicate autophagosomes, and the free red puncta indicate autolysosomes. Scale bar, 10 μm. **c** Immunofluorescence signals of cells double labeled with LC3-II (green) and LAMP1 (red). Scale bar, 10 μm. This figure, one-way ANOVA with post hoc comparisons by Tukey's multiple comparisons test was used. $*P<0.05$ compared with the control group. $\#P<0.05$ compared with the HG group. (Color figure online)

injury, as seen in Supplementary Fig. 3, HIF-1α silencing must block the protective effects of BDNF toward BMEC dysfunction under HG conditions, as evaluated by the cell viability assay, MDA content, SOD activity, and Bcl-2/Bax protein level ratio, further confirming that HIF-1α is regulated by BDNF.

Next, we detected the changes in BNIP3-mediated mitophagy in BMECs after BDNF exposure. BMECs were

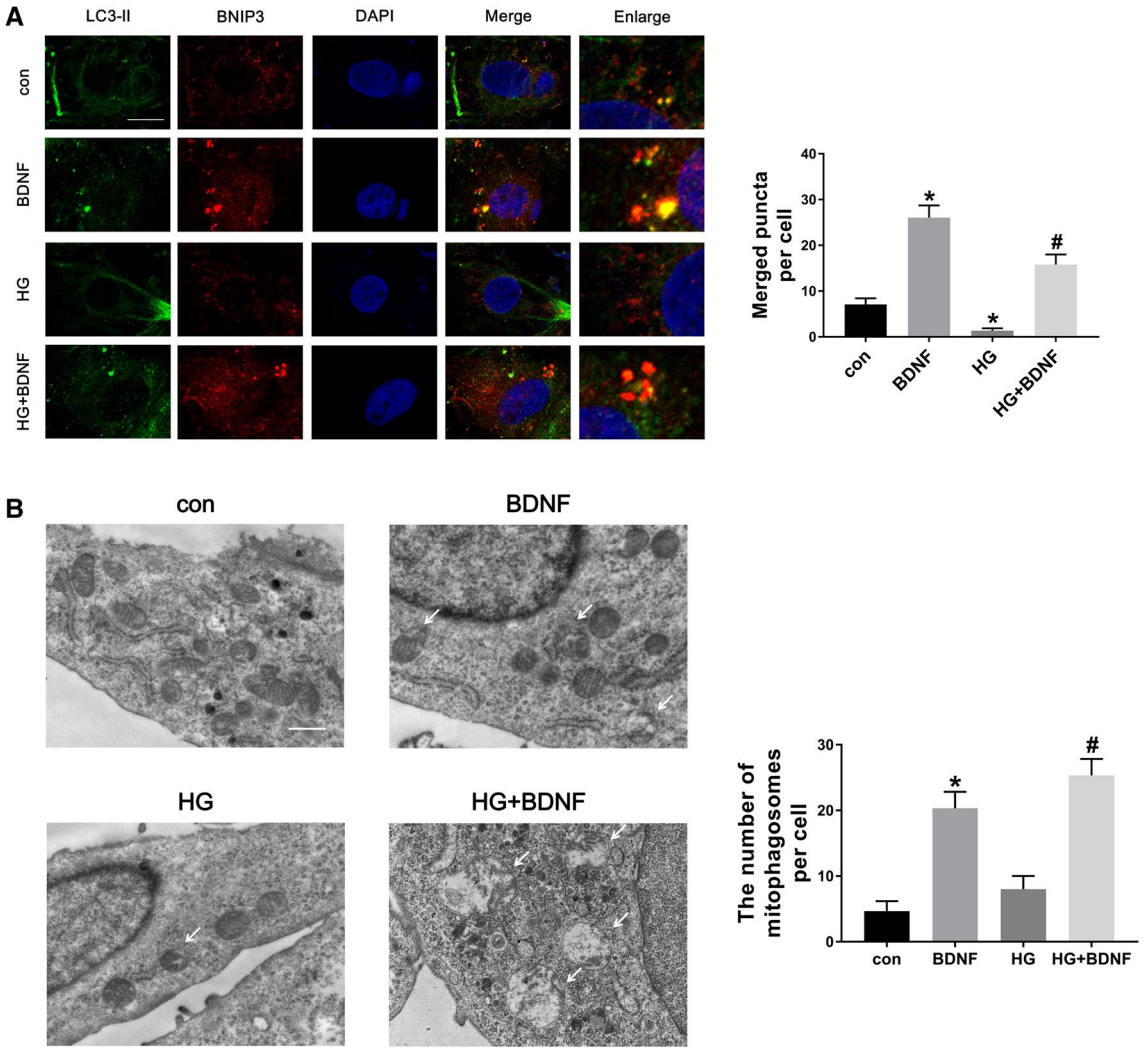

Fig. 6 BDNF induces mitophagy in BMECs. BMECs were treated with or without BDNF (100 ng/ml) in cells cultured under normal glucose or HG conditions. **a** BMECs were double stained to detect LC3-II (green) and BNIP3 (red). Scale bar, 10 μm. **b** Representative TEM photomicrographs showing the formation of mitophagosomes containing mitochondria fragments (white arrows). At least 6–8 cells per condition were imaged. The quantification results showed that the number of mitophagosomes was increased by the BDNF treatment (100 ng/ml). Scale bar, 1 μm. This figure, one-way ANOVA with post hoc comparisons by Tukey's multiple comparisons test was used. $^{*}P < 0.05$ compared with the control group. $\#P < 0.05$ compared with the HG group. (Color figure online)

transfected with siRNA against BNIP3 for 48 h, and the observed silencing efficiency was nearly 60% (Supplementary Fig. 2b). The results of TEM observations revealed the presence of fewer mitophagosomes (white arrows) in the BNIP3 knockdown group (Fig. 7d). Taken together, these results show that the BDNF/TrkB/HIF-1α/BNIP3 signaling pathway may induce mitophagy.

BNIP3-mediated mitophagy has a protective role in HG-induced BMEC dysfunction

Because BDNF enhanced mitophagy under HG conditions and because mitophagy has been reported to prevent cell damage in some instances [8, 9, 44], we assessed whether BNIP3-mediated mitophagy can alleviate intensive oxidative stress and cell apoptosis triggered by HG. No significant influence on intensive oxidative stress and cell apoptosis was observed for normal and HG cells after scrambled or targeted siRNA transfection (Date not shown). After BNIP3 was silenced using an appropriate siRNA, BMECs were treated with BDNF under HG conditions. The CCK-8 assay results indicated that BNIP3 knockdown decreased cell viability when compared with the scrambled siRNA group (Fig. 8a). In addition, BNIP3 silencing altered the antioxidative stress effects of BDNF, which was deduced by the observed intracellular ROS formation, SOD activity, MDA content, and NO content (Fig. 8b–e). Furthermore, BNIP3 silencing inhibited the protective effects of BDNF

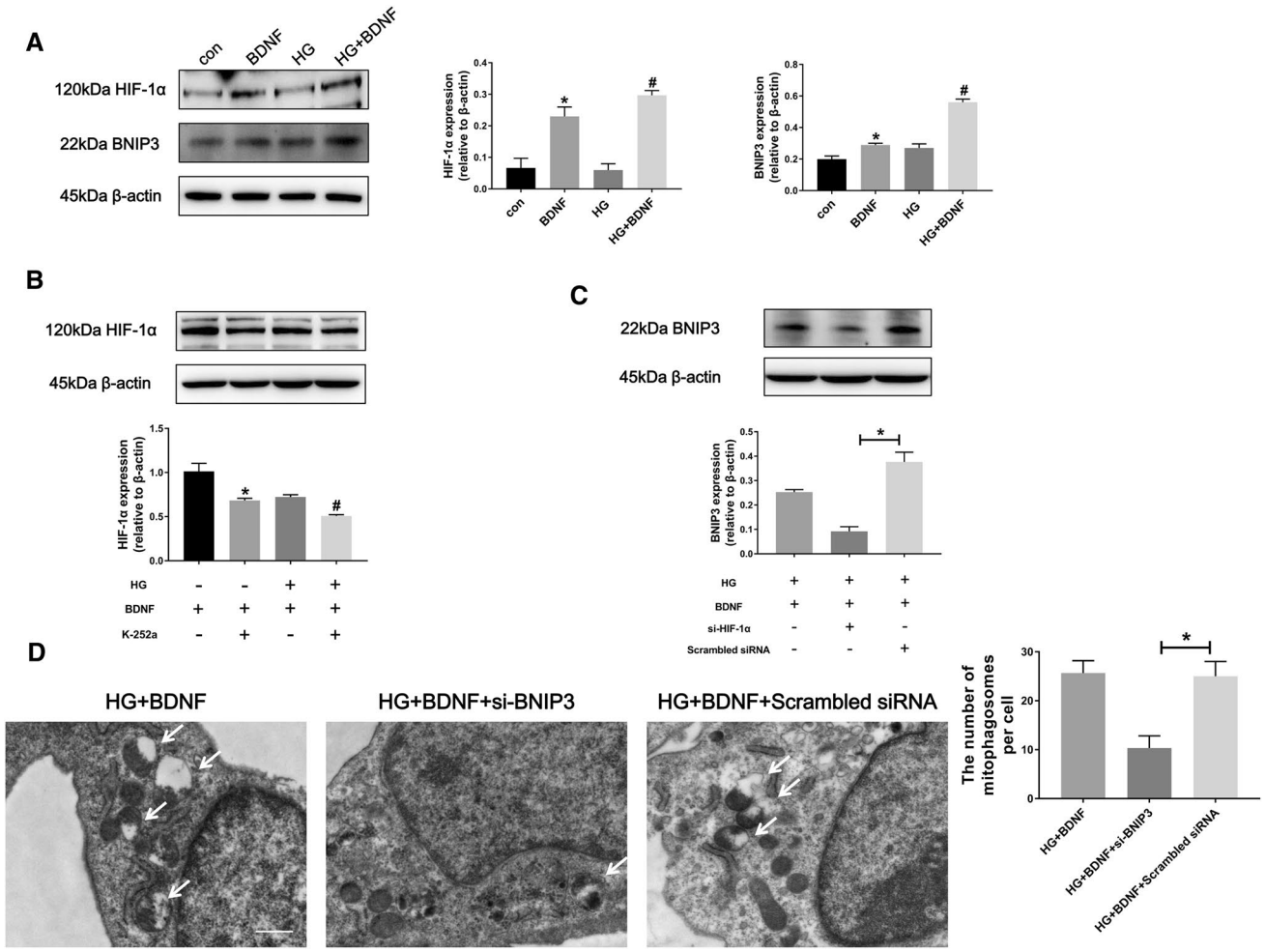

Fig. 7 HIF-1α/BNIP3 signaling occurs during BDNF/TrkB-activated mitophagy. **a** Western blot analysis of HIF-1α and BNIP3 expression with or without BDNF treatment (100 ng/ml) after cells were cultured under normal glucose or HG conditions. $*P<0.05$ compared with the control group. $\#P<0.05$ compared with the HG group. **b** BMECs were treated with K-252a (a potent TrkB receptor inhibitor) under normal glucose or HG culture conditions, and the HIF-1α protein level was determined by western blotting. $*P<0.05$ compared with the BDNF group. $\#P<0.05$ compared with the HG + BDNF group. **c** After transfection, the BNIP3 protein level was measured in cells cultured under HG conditions with or without BDNF (100 ng/ml). $*P<0.05$ vs. the indicated treatment. **d** Mitophagy was evaluated by assessing the formation of mitophagosomes (white arrows) in the TEM photomicrographs. The quantification results showed that the number of mitophagosomes decreased after BNIP3 knockdown. Scale bar, 1 μm. $*P<0.05$ versus the indicated treatment. This figure, one-way ANOVA with post hoc comparisons by Tukey's multiple comparisons test was used

toward BMEC early apoptosis under HG conditions as evaluated through an annexin V-FITC/PI double staining assay (Fig. 8f) and western blotting (Fig. 8g) after HG exposure. These results further demonstrate that BNIP3-mediated mitophagy can aid in preventing HG-induced BMEC injury.

Discussion

Endothelial cells ensure normal vessel contraction and relaxation and have specific functions, such as regulating blood pressure and maintaining the balance of coagulation and anticoagulation factors in blood [45]. The health of the brain microvascular endothelium is essential for cerebral circulatory system health [46]. Diabetes causes a great deal of damage to the brain microcirculatory system, and the results of previous studies have shown that BMECs are subjected to oxidative stress and apoptosis in diabetic environments, affecting the normal operation of the brain circulatory system [20, 21, 47]. Mitochondria are the primary sites for ROS production and are targets of oxidative damage [36]. Mitochondrial dysfunction serves as a central event in insulin resistance or hyperglycemia, resulting in an imbalance between inflammation and the elimination of ROS and ultimately triggering apoptotic and necrotic cell death [48]. Moreover, the damage inflicted upon

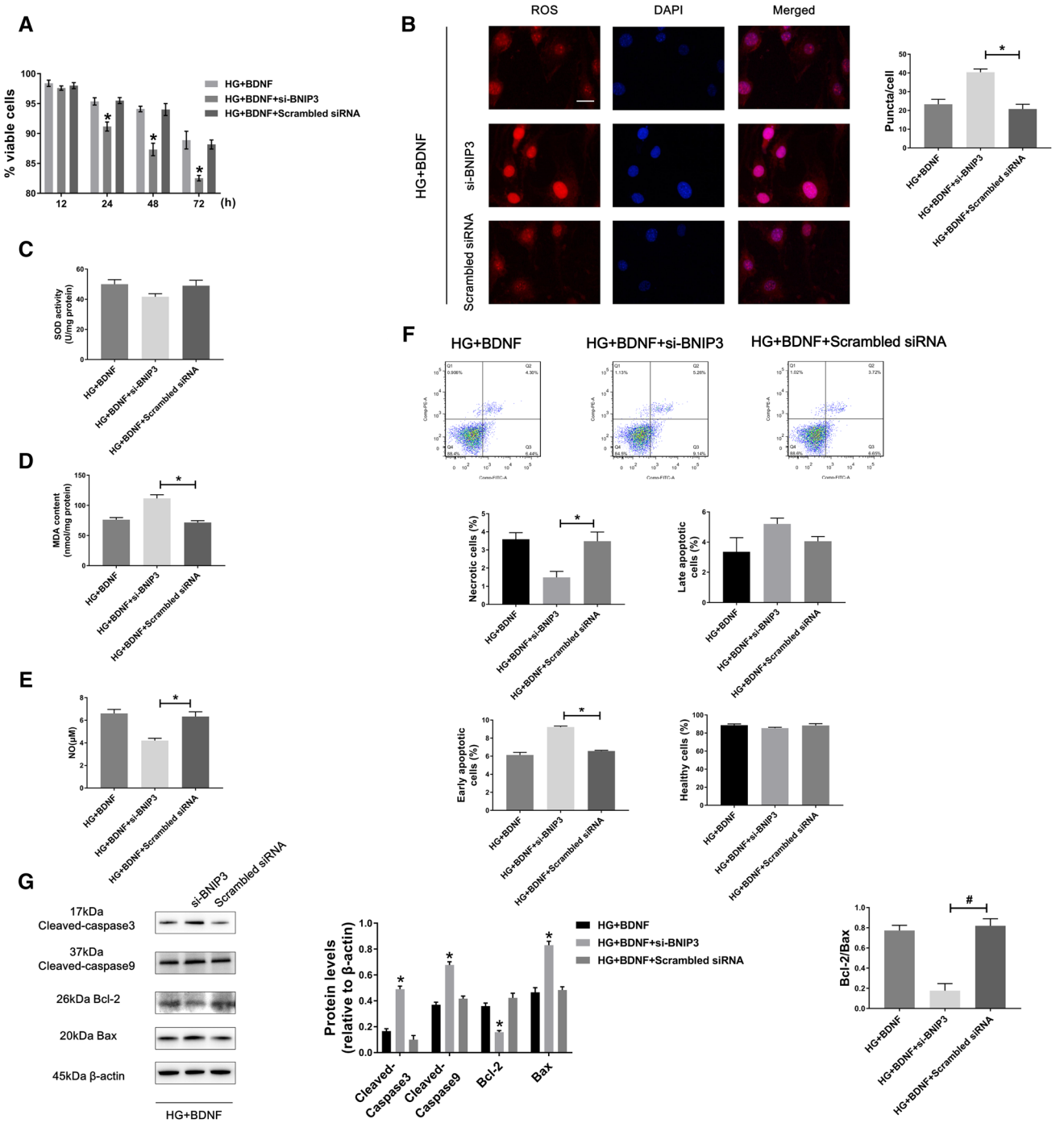

Fig. 8 BNIP3-mediated mitophagy deficiency alleviates the protective effect of BDNF toward BMEC dysfunction under HG conditions. BMECs were transfected with siRNA against BNIP3 or scrambled siRNA for 48 h and then treated with BDNF (100 ng/ml) under HG conditions. **a** Cell viability was assessed through a CCK-8 assay at different time points. $^{*}P<0.05$ compared with the HG + BDNF + scrambled siRNA group. **b–e** ROS production, SOD activity, MDA content, and NO content were determined. Scale bar, 10 μm. $^{*}P<0.05$ versus the indicated treatment. **f** Healthy, early apoptotic, late apoptotic, and necrotic cell populations were evaluated by annexin V-FITC/PI double staining $^{*}P<0.05$ vs. the indicated treatment. **g** Protein levels of apoptosis pathway-related proteins. $^{*}P<0.05$ compared with the HG + BDNF + scrambled siRNA group. $\#P<0.05$ versus the indicated treatment. For **a**, two-way ANOVA with post hoc comparisons by Tukey's multiple comparisons test was used. For **b–g**, one-way ANOVA with post hoc comparisons by Tukey's multiple comparisons test was used

mitochondria increases the permeability of the mitochondrial membrane, which leads to the release of cytochrome c and the activation of the mitochondrial apoptotic pathway [49]. Consistent with previous studies, we observed that HG disrupted the dynamic stability of mitochondrial fission and fusion, decreased mitochondrial mass and biogenesis, and caused mitochondrial dysfunction, which was followed by excessive ROS accumulation and BMEC apoptosis. Although drugs such as probucol [50] and venlafaxine [47] have been shown to inhibit oxidative stress and human BMEC apoptosis, only mitophagy can promote the removal of damaged and unnecessary mitochondria to fundamentally reduce intracellular ROS production.

The antihyperglycemia effect of BDNF/TrkB typically acts upon the nervous system. The results of a previous study showed that cerebral BDNF can attenuate diabetic hyperglycemia through an insulin-independent mechanism [51]. Liu et al demonstrated that BDNF can protect retinal neurons from hyperglycemia via the TrkB/extracellular signal-regulated kinase (ERK)/mitogen-activated protein kinase (MAPK) pathway [52]. However, there has been increasing interest in the role of BDNF/TrkB in blood vessels, as they are widely expressed in vascular endothelial cells [53]. In the diabetic brain, TrkB can be proteolytically degraded by advanced glycation end-product (AGE)-induced MMP9 activation, negating the protective effect of BDNF on brain microcirculation [21]. In addition, AGEs downregulate intracellular and secreted BDNF expression in human BMECs via the ERK/MAP pathway [20]. Endothelial NO can activate endothelial BDNF synthesis [54], and interestingly, exogenous BDNF causes a feedback resulting in the overproduction of NO [55]. Moreover, our group has shown that metformin, the first-line medication for T2DM treatment, can modulate human umbilical vein endothelial cell (HUVEC) proliferation and apoptosis under HG conditions via the AMP-activated protein kinase (AMPK)/cAMP response element-binding protein (CREB)/BDNF pathway [56] Collectively, upregulation of the BDNF/TrkB pathway is associated with vascular endothelial health. In this study, HG conditions caused decreased BDNF expression in BMECs and supernatants and inhibited BDNF nuclear translocation, which was consistent with previously observed changes in BDNF expression in human BMECs in a diabetic model [20]. As expected from the results of previous studies [20, 21, 50], BDNF exhibited a protective effect toward the brain microvascular endothelial system, greatly mitigating oxidative stress and apoptosis. Although pro-BDNF, a BDNF precursor that can be transformed into mature BDNF, has a proapoptotic effect toward myocardial microvascular endothelial cells [57]. The microvascular protective effect of BDNF has been demonstrated in several studies, and our study supported these results.

Autophagy involves the recycling of dysfunctional intracellular organelles to promote cellular homeostasis, and mitophagy is a specific type of autophagy that selectively eliminates damaged and unnecessary mitochondria [58]. To the best of our knowledge, this is the first study to demonstrate that BDNF can alleviate the block autophagy flux and mitophagy deficiencies in BMECs under hyperglycemia. Mitophagy is a protective mechanism that is induced by stress, including cellular ROS accumulation, mitochondrial swelling, mitochondrial membrane potential decline, and mitochondrial DNA damage [59], which is followed by clearance of injured mitochondria and the maintenance of homeostasis. In this study, we observed that BDNF alleviates mitochondrial dysfunction, although there are other links between BDNF and resistance to mitochondrial damage, such as the mPTP/pCREB/mitochondrial complex V pathway [60] and the NO/NF-κB/sestrin2 pathway [61]. We speculated that the final node of these pathways is mitophagy. We recently reported that in vascular smooth muscle cells, metformin-induced mitochondrial biogenesis is dependent on mitophagy signaling [62]. Interestingly, we observed that BDNF elevates mitochondrial biogenesis markers and mitochondrial mass, which had not been previously reported. Therefore, we speculated that BDNF-mediated mitochondrial biogenesis is also dependent on mitophagy. Aberrant mitochondrial accumulation increases oxygen consumption and ROS generation, which eventually results in oxidative stress and cell death [41]. However, these events were not detected in this study, suggesting a perfect balance of mitochondrial production and clearance after BDNF treatment.

Several studies have shown a connection between BDNF and autophagy [63–65], but few reports have detailed an association between BDNF and mitophagy, especially in hyperglycemia environments, and both autophagy and mitophagy were suppressed in response to HG treatment in our study. Diabetes is typically related to hypoxia, and HIF-1α expression was shown to be decreased in type 1 diabetes (T1DM) or T2DM [66–68]. In addition, BDNF/TrkB signaling increases VEGF in human chondrosarcoma cells, and VEGF is a downstream molecule of HIF-1α [69]. Furthermore, HIF-1α plays an important role in mitophagy, especially BNIP3-mediated mitophagy [70, 71]. Based on these studies, we examined HIF-1α as a potential bridge between BDNF/TrkB signaling and BNIP3-mediated mitophagy. Although autophagy and BNIP3-induced mitophagy were inhibited in the HG state, BDNF activated downstream signaling molecules to induce autophagy and mitophagy. Although we have not directly demonstrated that mitochondrial biogenesis is dependent on mitophagy, the anti-oxidative stress and apoptosis effects of BDNF/HIF-1α/BNIP3/mitophagy have been discovered. Therefore, we believed that the protective effects of BDNF in HG

stress environment depend in part on damaged mitochondrial clearance. To date, three mechanisms of mitophagy have been widely investigated: BNIP3-related mitophagy, the PTEN-induced putative kinase 1 (PINK1)/parkin pathway, and FUN14 domain containing 1 (FUNDC1)-mediated mitophagy. The latter two pathways are also modulated by HIF-1α, and their relationship with BDNF requires further study.

As another important circulatory organ, the heart is a highly structured organ consisting of different cell types, including cardiomyocytes, endothelial cells, fibroblasts, stem cells, and inflammatory cells. MECs are also widely studied in the heart system. However, unlike investigations of BMECs, in addition to focusing on the cell damage and self-regulation under pathological conditions, such as diabetes and ischemia–reperfusion injury, more investigations of MECs have focused on cell-to-cell interactions. For example, MECs transform into cardiomyocytes, and MECs act on other cells by paracrine signaling [72–75]. In our study, BMECs were observed to secrete the protective protein BDNF, and whether BDNF promotes various biological effects through cell-to-cell interactions is a direction of future research.

Our study had some limitations. First, the use of two vectors in the experimental design of the HIF-1α and BNIP3 silencing assays would have increased the rigorousness of the results. Second, because diabetes is a chronic disease and short-term high glucose damage to endothelial cells can not completely mimic diabetic endothelial injury, in vivo studies should be performed in future research. Finally, in diabetes, one of the affected organs is the eye. Specifically, retinal ischemia and hemorrhaging are hallmarks of worsening diabetic retinopathy, which can lead to neovascularization, macular edema, and severe vision loss [76]. Increased VEGF can promote neovascularization, worsening diabetic retinal ischemia. In this instance, the use of BDNF is contradictory, and how to avoid damage to diabetic retinopathy also requires further investigation.

Conclusions

In summary, the results of this study demonstrated that BDNF can alleviate mitochondrial dysfunction, oxidative stress and apoptosis in BMECs under hyperglycemic conditions. Through BNIP3-related mitophagy, BNDF was shown to maintain a dynamic balance between mitochondrial clearance and biogenesis. In addition, we confirmed that HIF-1α is associated with BDNF/TrkB-induced mitophagy. Furthermore, BDNF-induced mitophagy was shown to promote antioxidative stress and apoptosis. Taken together, BDNF/TrkB/HIF-1α/BNIP3-mediated mitophagy prevents BMEC dysfunction under hyperglycemic conditions, further enriching our understanding of the role of mitophagy in cardiovascular disease. Furthermore, the protective effect of BDNF on the cerebrovascular endothelium could be a novel target for the treatment of diabetic cerebrovascular complications.

Acknowledgements This work was supported by the Fundamental Research Funds for the Central Universities and Postgraduate Research & Practice Innovation Program of Jiangsu Province (No. KYCX17_0174) and the Jiangsu Provincial Health and Wellness Committee Research Project (No. H2018001).

Compliance with ethical standards

Conflict of interest The authors have no conflicts of interest.

References

1. Schiel R, Stachow R, Hermann T et al (2018) Rehabilitation in Germany 2004–2016 A Multicenter Analysis Over a Period of 13 Years in Children and Adolescents with Diabetes Mellitus. Experimental and clinical endocrinology & diabetes: official journal, German Society of Endocrinology [and] German Diabetes Association
2. Xu R, Yang R, Hu H, Xi Q, Wan H, Wu Y (2013) Diabetes alters the expression of partial vasoactivators in cerebral vascular disease susceptible regions of the diabetic rat. Diabetol Metab Syndr 5:63
3. Cantu-Brito C, Mimenza-Alvarado A, Sanchez-Hernandez JJ (2010) Diabetes mellitus and aging as a risk factor for cerebral vascular disease: epidemiology, pathophysiology and prevention. Revista de investigacion clinica 62:333–342
4. Ergul A, Abdelsaid M, Fouda AY, Fagan SC (2014) Cerebral neovascularization in diabetes: implications for stroke recovery and beyond. J Cereb Blood Flow Metab 34:553–563
5. Li H, Gao A, Feng D et al (2014) Evaluation of the protective potential of brain microvascular endothelial cell autophagy on blood-brain barrier integrity during experimental cerebral ischemia-reperfusion injury. Transl Stroke Res 5:618–626
6. Guo S, Deng W, Xing C, Zhou Y, Ning M, Lo EH (2018) Effects of aging, hypertension and diabetes on the mouse brain and heart vasculomes. Neurobiol Dis. https://doi.org/10.1016/j.nbd.2018.07.021
7. Guan G, Han H, Yang Y, Jin Y, Wang X, Liu X (2014) Neferine prevented hyperglycemia-induced endothelial cell apoptosis through suppressing ROS/Akt/NF-kappaB signal. Endocrine 47:764–771
8. Zhao Y, Huang S, Liu J et al (2018) Mitophagy contributes to the pathogenesis of inflammatory diseases. Inflammation 41(5):1590–1600
9. Di Rita A, D'Acunzo P, Simula L, Campello S, Strappazzon F, Cecconi F (2018) AMBRA1-mediated mitophagy counteracts oxidative stress and apoptosis induced by neurotoxicity in human neuroblastoma SH-SY5Y cells. Front Cell Neurosci 12:92
10. Lohitesh K, Saini H, Srivastava A, Mukherjee S, Roy A, Chowdhury R (2018) Autophagy inhibition potentiates SAHAmediated apoptosis in glioblastoma cells by accumulation of damaged mitochondria. Oncol Rep 39:2787–2796
11. Chakrabarty S, Kabekkodu SP, Singh RP, Thangaraj K, Singh KK, Satyamoorthy K (2018) Mitochondria in health and disease. Mitochondrion 43:25–29

12. Abdelwahid E, Stulpinas A, Kalvelyte A (2017) Effective agents targeting the mitochondria and apoptosis to protect the heart. Curr Pharm Des 23:1153–1166
13. Thangaraj A, Periyasamy P (2018) HIV-1 TAT-mediated microglial activation: role of mitochondrial dysfunction and defective mitophagy. Autophagy 14(9):1596–1619.
14. Lan R, Wu JT, Wu T et al (2018) Mitophagy is activated in brain damage induced by cerebral ischemia and reperfusion via the PINK1/Parkin/p62 signalling pathway. Brain Res Bull 142:63–77
15. Marshall J, Zhou XZ, Chen G et al (2018) Antidepression action of BDNF requires and is mimicked by Galphai1/3 expression in the hippocampus. 115:e3549–e3558
16. Eyileten C, Zaremba M, Janicki PK et al (2016) Serum brain-derived neurotrophic factor is related to platelet reactivity but not to genetic polymorphisms within BDNF encoding gene in patients with type 2 diabetes. Med Sci Monit 22:69–76
17. Li B, Lang N, Cheng ZF (2016) Serum levels of brain-derived neurotrophic factor are associated with diabetes risk, complications, and obesity: a cohort study from chinese patients with type 2 diabetes. Mol Neurobiol 53:5492–5499
18. Jin H, Chen Y, Wang B et al (2018) Association between brain-derived neurotrophic factor and von Willebrand factor levels in patients with stable coronary artery disease. BMC Cardiovasc Disord 18:23
19. Wood J, Tse MCL, Yang X et al (2018) BDNF mimetic alleviates body weight gain in obese mice by enhancing mitochondrial biogenesis in skeletal muscle. Metabolism 87:113–122
20. Navaratna D, Guo SZ, Hayakawa K, Wang X, Gerhardinger C, Lo EH (2011) Decreased cerebrovascular brain-derived neurotrophic factor-mediated neuroprotection in the diabetic brain. Diabetes 60:1789–1796
21. Navaratna D, Fan X, Leung W et al (2013) Cerebrovascular degradation of TRKB by MMP9 in the diabetic brain. J Clin Invest 123:3373–3377
22. Huang C, Zhang Y, Kelly DJ et al (2016) Thioredoxin interacting protein (TXNIP) regulates tubular autophagy and mitophagy in diabetic nephropathy through the mTOR signaling pathway. Sci Rep 6:29196
23. Nakamura K, Martin KC, Jackson JK, Beppu K, Woo CW, Thiele CJ (2006) Brain-derived neurotrophic factor activation of TrkB induces vascular endothelial growth factor expression via hypoxia-inducible factor-1alpha in neuroblastoma cells. Cancer Res 66:4249–4255
24. Gao Y, Jing M, Ge R, Lang L (2016) Induction of hypoxia-inducible factor-1alpha by BDNF protects retinoblastoma cells against chemotherapy-induced apoptosis. Molecular cellular biochemistry 414:77–84
25. Feng CC, Lin CC, Lai YP et al (2016) Hypoxia suppresses myocardial survival pathway through HIF-1alpha-IGFBP-3-dependent signaling and enhances cardiomyocyte autophagic and apoptotic effects mainly via FoxO3a-induced BNIP3 expression. Growth Factors (Chur. Switzerland) 34:73–86
26. Wu H, Huang S, Chen Z, Liu W, Zhou X, Zhang D (2015) Hypoxia-induced autophagy contributes to the invasion of salivary adenoid cystic carcinoma through the HIF-1alpha/BNIP3 signaling pathway. Mol Med Rep 12:6467–6474
27. Hsieh DJ, Kuo WW, Lai YP et al (2015) 17beta-Estradiol and/or estrogen receptor beta attenuate the autophagic and apoptotic effects induced by prolonged hypoxia through HIF-1alpha-mediated BNIP3 and IGFBP-3 signaling blockage. Cell Physiol Biochem 36:274–284
28. Thongchot S, Yongvanit P, Loilome W et al (2014) High expression of HIF-1alpha, BNIP3 and PI3KC3: hypoxia-induced autophagy predicts cholangiocarcinoma survival and metastasis. Asian Pacific J Cancer Prev 15:5873–5878
29. Rui L, Weiyi L, Yu M et al (2018) The serine/threonine protein kinase of Streptococcus suis serotype 2 affects the ability of the pathogen to penetrate the blood-brain barrier. Cell Microbiol 20:e12862
30. Zhu X, Zhou Y, Cai W, Sun H, Qiu L (2017) Salusin-beta mediates high glucose-induced endothelial injury via disruption of AMPK signaling pathway. Biochem Biophys Res Commun 491:515–521
31. Fiorentino TV, Prioletta A, Zuo P, Folli F (2013) Hyperglycemia-induced oxidative stress and its role in diabetes mellitus related cardiovascular diseases. Curr Pharm Des 19:5695–5703
32. Elmore S (2007) Apoptosis: a review of programmed cell death. Toxicol Pathol 35:495–516
33. Rigothier C, Saleem MA, Bourget C, Mathieson PW, Combe C, Welsh GI (2016) Nuclear translocation of IQGAP1 protein upon exposure to puromycin aminonucleoside in cultured human podocytes: ERK pathway involvement. Cell Signal 28:1470–1478
34. Chavez-Valdez R, Martin LJ, Razdan S, Gauda EB, Northington FJ (2014) Sexual dimorphism in BDNF signaling after neonatal hypoxia-ischemia and treatment with necrostatin-1. Neuroscience 260:106–119
35. Wessels JM, Wu L, Leyland NA, Wang H, Foster WG (2014) The brain-uterus connection: brain derived neurotrophic factor (BDNF) and its receptor (Ntrk2) are conserved in the mammalian uterus. PloS one 9:e94036
36. Angelova PR, Abramov AY (2018) Role of mitochondrial ROS in the brain: from physiology to neurodegeneration. FEBS Lett 592:692–702
37. Yu T, Dohl J, Chen Y, Gasier HG, Deuster PA (2019) Astaxanthin but not quercetin preserves mitochondrial integrity and function, ameliorates oxidative stress, and reduces heat-induced skeletal muscle injury. J Cell Physiol. https://doi.org/10.1002/jcp.28006
38. Kubli DA, Gustafsson AB (2012) Mitochondria and mitophagy: the yin and yang of cell death control. Circ Res 111:1208–1221
39. Anne Stetler R, Leak RK, Gao Y, Chen J (2013) The dynamics of the mitochondrial organelle as a potential therapeutic target. J Cereb Blood Flow Metab 33:22–32
40. Eyileten C, Kaplon-Cieslicka A, Mirowska-Guzel D (2017) Antidiabetic effect of brain-derived neurotrophic factor and its association with inflammation in type 2. Diabetes Mellit. 2017:2823671
41. Palikaras K, Tavernarakis N (2014) Mitochondrial homeostasis: the interplay between mitophagy and mitochondrial biogenesis. Exp Gerontol 56:182–188
42. Suzuki S, Koshimizu H, Adachi N et al (2017) Functional interaction between BDNF and mGluR II in vitro: BDNF down-regulated mGluR II gene expression and an mGluR II agonist enhanced BDNF-induced BDNF gene expression in rat cerebral cortical neurons. Peptides 89:42–49
43. Bathina S, Srinivas N, Das UN (2016) BDNF protects pancreatic beta cells (RIN5F) against cytotoxic action of alloxan, streptozotocin, doxorubicin and benzo(a)pyrene in vitro. Metabolism 65:667–684
44. Xiong W, Hua J, Liu Z et al (2018) PTEN induced putative kinase 1 (PINK1) alleviates angiotensin II-induced cardiac injury by ameliorating mitochondrial dysfunction. Int J Cardiol 266:198–205
45. Del Papa N, Pignataro F (2018) The role of endothelial progenitors in the repair of vascular damage in systemic sclerosis. Front Immunol 9:1383
46. Fang L, Li X, Zhong Y et al (2015) Autophagy protects human brain microvascular endothelial cells against methylglyoxal-induced injuries, reproducible in a cerebral ischemic model in diabetic rats. J Neurochem 135:431–440
47. Lv Q, Gu C, Chen C (2014) Venlafaxine protects methylglyoxal-induced apoptosis in the cultured human brain microvascular endothelial cells. Neurosci Lett 569:99–103

48. Kang J, Jia Z, Ping Y et al (2018) Testosterone alleviates mitochondrial ROS accumulation and mitochondria-mediated apoptosis in the gastric mucosa of orchiectomized rats. Arch Biochem Biophys 649:53–59
49. Zhou J, Wang H, Shen R et al (2018) Mitochondrial-targeted antioxidant MitoQ provides neuroprotection and reduces neuronal apoptosis in experimental traumatic brain injury possibly via the Nrf2-ARE pathway. Am J Transl Res 10:1887–1899
50. Ma J, Zhao S, Gao G, Chang H, Ma P, Jin B (2015) Probucol protects against asymmetric dimethylarginine-induced apoptosis in the cultured human brain microvascular endothelial cells. J Mol Neurosci 57:546–553
51. Meek TH, Wisse BE, Thaler JP et al (2013) BDNF action in the brain attenuates diabetic hyperglycemia via insulin-independent inhibition of hepatic glucose production. Diabetes 62:1512–1518
52. Liu Y, Tao L, Fu X, Zhao Y, Xu X (2013) BDNF protects retinal neurons from hyperglycemia through the TrkB/ERK/MAPK pathway. Mol Med Rep 7:1773–1778
53. Jiang H, Huang S, Li X, Li X, Zhang Y, Chen ZY (2015) Tyrosine kinase receptor B protects against coronary artery disease and promotes adult vasculature integrity by regulating Ets1-mediated VE-cadherin expression. Arterioscler Thromb Vasc Biol 35:580–588
54. Monnier A, Prigent-Tessier A, Quirie A et al (2017) Brain-derived neurotrophic factor of the cerebral microvasculature: a forgotten and nitric oxide-dependent contributor of brain-derived neurotrophic factor in the brain. Acta Physiolo (Oxford England) 219:790–802
55. Meuchel LW, Thompson MA, Cassivi SD, Pabelick CM, Prakash YS (2011) Neurotrophins induce nitric oxide generation in human pulmonary artery endothelial cells. Cardiovasc Res 91:668–676
56. Han X, Wang B, Sun Y et al (2018) Metformin modulates high glucose-incubated human umbilical vein endothelial cells proliferation and apoptosis through AMPK/CREB/BDNF pathway. Front Pharmacol 9:1266
57. Yu F, Liu Y, Xu J (2018) Pro-BDNF contributes to hypoxia/reoxygenation injury in myocardial microvascular endothelial cells: roles of receptors p75(NTR) and sortilin and activation of JNK and Caspase 3. 2018:3091424
58. Saito T, Sadoshima J (2015) Molecular mechanisms of mitochondrial autophagy/mitophagy in the heart. Circ Res 116:1477–1490
59. Liu L, Sakakibara K, Chen Q, Okamoto K (2014) Receptor-mediated mitophagy in yeast and mammalian systems. Cell Res 24:787–795
60. Xu Z, Lv XA, Dai Q, Lu M, Jin Z (2018) Exogenous BDNF increases mitochondrial pCREB and alleviates neuronal metabolic defects following mechanical injury in a MPTP-dependent way. Mol Neurobiol 55:3499–3512
61. Wu CL, Chen SD, Yin JH, Hwang CS, Yang DI (2016) Nuclear factor-kappaB-dependent Sestrin2 induction mediates the antioxidant effects of BDNF against mitochondrial inhibition in rat cortical neurons. Mol Neurobiol 53:4126–4142
62. Ma WQ, Sun XJ, Wang Y, Zhu Y, Han XQ, Liu NF (2018) Restoring mitochondrial biogenesis with metformin attenuates beta-GP-induced phenotypic transformation of VSMCs into an osteogenic phenotype via inhibition of PDK4/oxidative stress-mediated apoptosis. Mol Cell Endocrinol, 479:39–53
63. Nikoletopoulou V, Sidiropoulou K, Kallergi E, Dalezios Y, Tavernarakis N (2017) Modulation of autophagy by BDNF underlies synaptic plasticity. Cell Metab 26:230–242.e235
64. Song X, Liu B, Cui L et al (2017) Silibinin ameliorates anxiety/depression-like behaviors in amyloid beta-treated rats by upregulating BDNF/TrkB pathway and attenuating autophagy in hippocampus. Physiol Behav 179:487–493
65. Mazouffre C, Geyl S, Perraud A et al (2017) Dual inhibition of BDNF/TrkB and autophagy: a promising therapeutic approach for colorectal cancer. 21:2610–2622
66. Catrina SB (2014) Impaired hypoxia-inducible factor (HIF) regulation by hyperglycemia. J Mol Med (Berlin Germany) 92:1025–1034
67. Yu WY, Sun W, Yu DJ, Zhao TL, Wu LJ, Zhuang HR (2018) Adipose-derived stem cells improve neovascularization in ischemic flaps in diabetic mellitus through HIF-1alpha/VEGF pathway. Eur Rev Med Pharmacol Sci 22:10–16
68. Krishan P, Singh G, Bedi O (2017) Carbohydrate restriction ameliorates nephropathy by reducing oxidative stress and upregulating HIF-1alpha levels in type-1 diabetic rats. J Diabetes Metab Disorders 16:47
69. Lin CY, Hung SY, Chen HT et al (2014) Brain-derived neurotrophic factor increases vascular endothelial growth factor expression and enhances angiogenesis in human chondrosarcoma cells. Biochem Pharmacol 91:522–533
70. Chourasia AH, Tracy K, Frankenberger C et al (2015) Mitophagy defects arising from BNip3 loss promote mammary tumor progression to metastasis. EMBO Rep 16:1145–1163
71. Song J, Yoon D, Christensen RD, Horvathova M, Thiagarajan P, Prchal JT (2015) HIF-mediated increased ROS from reduced mitophagy and decreased catalase causes neocytolysis. J Mol Med (Berlin Germany) 93:857–866
72. Segers VFM, Brutsaert DL, De Keulenaer GW (2018) Cardiac remodeling: endothelial cells have more to say than just NO. Front Physiol 9:382
73. Hu J, Wang S, Xiong Z et al (2018) Exosomal Mst1 transfer from cardiac microvascular endothelial cells to cardiomyocytes deteriorates diabetic cardiomyopathy. Biochim Biophys Acta Mol Basis Dis 1864:3639–3649
74. Sniegon I, Priess M, Heger J, Schulz R, Euler G (2017) Endothelial mesenchymal transition in hypoxic microvascular endothelial cells and paracrine induction of cardiomyocyte apoptosis are mediated via TGFbeta(1)/SMAD signaling. Int J Mol Sci 18:2290
75. Wang F, Jia J, Lal N et al (2016) High glucose facilitated endothelial heparanase transfer to the cardiomyocyte modifies its cell death signature. Cardiovasc Res 112:656–668
76. Duh EJ, Sun JK, Stitt AW (2017) Diabetic retinopathy: current understanding, mechanisms, and treatment strategies. JCI Insight 2